

# Challenging the paradigm of singularity excision in gravitational collapse

Luca Baiotti<sup>1</sup>, Luciano Rezzolla<sup>1,2,3</sup>

<sup>1</sup>*Max-Planck-Institut für Gravitationsphysik, Albert-Einstein-Institut, 14476 Golm, Germany*

<sup>2</sup>*SISSA, International School for Advanced Studies and INFN, Via Beirut 2, 34014 Trieste, Italy* and

<sup>3</sup>*Department of Physics, Louisiana State University, Baton Rouge, LA 70803 USA*

(Dated: December 2, 2024)

A paradigm deeply rooted in modern numerical relativity calculations prescribes the removal of those regions of the computational domain where a physical singularity may develop. We here challenge this paradigm by performing three-dimensional simulations of the collapse of uniformly rotating stars to black holes without excision. We show that this choice, combined with suitable gauge conditions and the use of minute numerical dissipation, improves dramatically the long-term stability of the evolutions. In turn, this allows for the calculation of the waveforms well beyond what previously possible, providing information on the black-hole ringing and setting a new mark on the present knowledge of the gravitational-wave emission from the stellar collapse to a rotating black hole.

PACS numbers: 04.25.Dm, 04.30.Db, 04.70.Bw, 95.30.Lz, 97.60.Jd

Numerical relativity simulations have recently recorded important breakthroughs, which have allowed for long-term stable and accurate calculations of curved and highly dynamical spacetimes, thus increasing their potential of providing physically relevant predictions for gravitational-wave astronomy. Behind this rapid progress are various novel approaches, some of which involve the dropping of assumptions or techniques that were considered to be important or simply necessary. Firstly, the dismissal of the 3+1 ADM formulation of the field equations, which, after large-scale efforts [1], has shown not to have the stability properties necessary for long-term fully three-dimensional (3D) simulations. In lieu of the ADM equations, new formulations have been either reconsidered (as in the case of the conformal and traceless formulation of the ADM equations [2]) or investigated for the first time in 3D simulations (as in the case of the harmonic formulation of the Einstein equations [3]). Both approaches have been shown to provide long-term stability on timescales sufficiently large to evolve accurately a large class of spacetimes, including black holes [3, 4, 5] and neutron stars [6, 7]. Secondly, the abandoning of the use of numerical grids with uniform spacing, in lieu of which several codes now use mesh-refinement techniques (either fixed [8] or with adaptivity [4]). This conceptually simple but technologically challenging improvement allows to concentrate computational resources where the truncation error needs to be the smallest, while saving them where they may not be needed. In turn, non-uniform grids have allowed to place the outer boundaries of the computational domain at very large distances, thus reducing the influence of inaccurate outer-boundary conditions and making it possible to have the wave-zone within the domain and to extract there the precious gravitational-wave signal [9]. Thirdly, for some years now, successful long-term 3D evolutions of black-hole vacuum spacetimes have been possible only thanks to the use of excision techniques (see, *e.g.*, [10] for a first example), that is by ignoring the spacetime regions inside black-hole horizons. These are causally disconnected from the outside and should have no effect on the rest of the evolution as long as

a suitable treatment of the equations is made at the excision surface. Furthermore, recent simulations of the collapse of rotating neutron stars to Kerr black holes [7, 11] have shown the effectiveness of excision techniques also for spacetimes with matter, where they were applied separately to the field equations and to the hydrodynamical equations. In those simulations, in fact, the use of excision has extended considerably the lifetime of the simulations, allowing for an accurate investigation of the dynamics of the trapped surfaces formed during the collapse and for the extraction of the first gravitational waveforms from 3D collapse to rotating black holes [9].

Although the assumption that a region of spacetime that is causally disconnected can be ignored without this affecting the solution in the remaining portion of the spacetime is certainly true for signals and perturbations travelling at physical speeds, numerical signals, such as gauge waves or constraint violations, may travel at velocities larger than that of light and thus leave the physically disconnected region. Indeed, this is what is commonly observed when excising a topologically spherical surface in Cartesian coordinates within a conformal and traceless formulation of the Einstein equations and without the massive use of numerical dissipation as in ref. [3].

In this paper we challenge the paradigm of singularity excision and show that accurate numerical simulations can be carried out even in the absence of an excised region and independently of whether the spacetime is vacuum and the singularity modelled as a “puncture” [4, 5]. In addition, we show that the absence of an excised region improves dramatically the long-term stability, allowing for the calculation of the gravitational waveforms well beyond what previously possible and past the black-hole quasi-normal-mode (QNM) ringing.

The simplest and most impressive way of proving the improvements resulting from not excising the region inside the apparent horizon (AH) is by reconsidering the same initial data of ref. [9], which lead to gravitational collapse to rotating black holes. More specifically, we consider rotating relativistic stars calculated as equilibrium solutions of the Einstein equations, with a polytropic equation of state  $p = K\rho^\Gamma$ ,

with  $\Gamma = 2$  and with the polytropic constant initially set to  $K_{\text{ID}} = 100$  [24]. To illustrate the gravitational collapse for the range of neutron stars rotating either very slowly or near the mass-shedding limit, we consider two representative models, indicated as D1 and D4 in ref. [11], with different initial angular momenta. The first one is a slowly rotating star of mass  $M = 1.67 M_{\odot}$ , circumferential equatorial radius  $R_e = 11.43$  km and  $a \equiv J/M^2 = 0.21$ , where  $J$  is the stellar angular momentum; the second one is a star with  $M = 1.86 M_{\odot}$ ,  $R_e = 14.25$  km and rotating close to the mass-shedding limit with  $a = 0.54$  (cf. Table I of [11]).

The numerical methods used for these evolutions are the same as discussed in ref. [9]. In particular, we use a conformal and traceless formulation of the ADM equations [12], which are solved with fourth-order finite-difference operators, while we evolve the hydrodynamical equations with the Whisky code [13], implementing high-resolution shock-capturing (HRSC) techniques with a variety of approximate Riemann solvers and reconstruction algorithms and an overall second-order truncation error [11]. The numerical grid setup makes use of the same mesh refinement implemented in the numerical infrastructure described in ref. [8]. Besides a fixed number of refinement levels which are present already on the initial slice, new refined levels are added at predefined positions and times during the evolution. More specifically, as the star collapses, the innermost (most refined) grid-box is progressively further refined with box-in-box grids, the final one having a resolution of  $\Delta x \simeq 0.02 M$ ; the outermost grid, instead, which is not further refined, has a resolution of  $\Delta x \simeq 1.5 M$ , sufficient to capture the details of the gravitational radiation. In this way, our outer boundaries are placed at  $\simeq 165 M$ , so as to minimize the influence of our imperfect outer-boundary conditions on the very small gravitational-wave signal. We note that the “switching-on” of different levels of resolution as the star collapses does have a small but appreciable effect on its dynamics, essentially due to the necessary interpolation to the new refined grids, which also changes the growth-time of the most unstable, exponentially growing mode. This effect is hardly noticeable in the evolution of the matter but can influence the waveforms. In order to provide a direct comparison with the previous studies [9], we have here followed the same approach.

Fig. 1 summarises the dynamics of the matter for model D4 by showing the time evolution of the maximum of the rest-mass density  $\rho_{\text{max}}$  (continuous lines) and of the total rest-mass  $M_*$  (dashed lines) when normalized to their initial values (a similar behaviour is observed also for the slowly rotating model D1). The evolution obtained without excision is to be contrasted with the one in which the excision is made (which is described in detail in ref. [14]) and which is indicated with thick lines. In that case, the excision was started soon after an AH [15] was found (this is marked with circles on the two curves) and the corresponding evolution terminated at  $t \gtrsim 77 M$ , when the code crashed with large violations in the Hamiltonian constraint. Note that while the maximum values for the rest-mass density attained during the evolution are

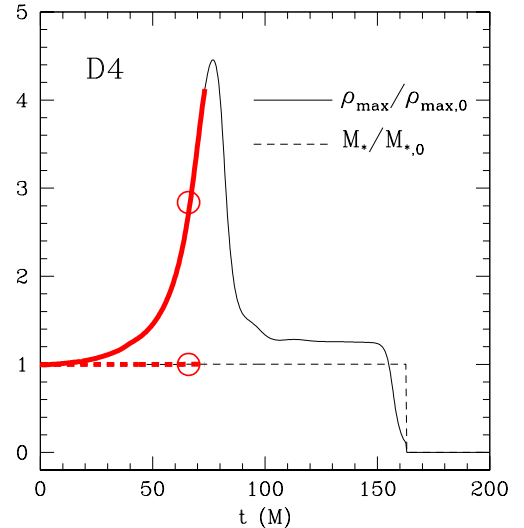


FIG. 1: Evolution of the normalized maximum of the rest-mass density  $\rho_{\text{max}}$  (continuous line) and of the total rest-mass  $M_*$  (dashed line) for model D4. Indicated with circles are the times at which the AH is first found and shown with thick lines are the corresponding results obtained with the use of the excision technique.

comparable in the two cases, the evolution without excision can be carried out to much later times (*i.e.*  $t \gtrsim 300 M$ ) without appreciable loss of accuracy or sign of instability. Indeed, as the matter collapses and concentrates over a very few grid-points (and ultimately on only one), the high accuracy of the HRSC methods is able to conserve the rest mass to very high precision with a loss of less than 0.2% up to when the narrowly peaked rest-mass density distribution is diffused as a result of the poorly resolved gradients.

While very little extra is needed for the evolution of the hydrodynamical quantities in the absence of an excision algorithm, a stable evolution of the Einstein equations requires at least two important ingredients. The first one is represented by gauge conditions for the lapse function  $\alpha$  with suitable singularity-avoidance properties. Our experience has shown that hyperbolic  $K$ -driver slicing conditions of the form  $\partial_t \alpha = -f(\alpha) \alpha^2 (K - K_0)$ , with  $f > 0$  and  $K_0$  being the trace of the extrinsic curvature at  $t = 0$ , are essential to “freeze” the evolution in those regions of the computational domain inside the AH, where the metric functions experience the growth of very large gradients. In practice, we confirm that using the generalized “1+log” slicing condition [16] as obtained by setting  $f = 2/\alpha$  provides the desired singularity avoidance and is computationally efficient [17]. With a good choice for the slicing condition, the results do not depend sensitively on the gauge condition for the shift. We have found that the use of the “Gamma-driver” shift conditions discussed in ref. [11] is sufficient to compensate for the “slice-stretching” induced by the singularity-avoiding slicing.

The second important ingredient is the introduction of an artificial dissipation of the Kreiss-Oliger type [18] on the right-hand-sides of the evolution equations for the spacetime

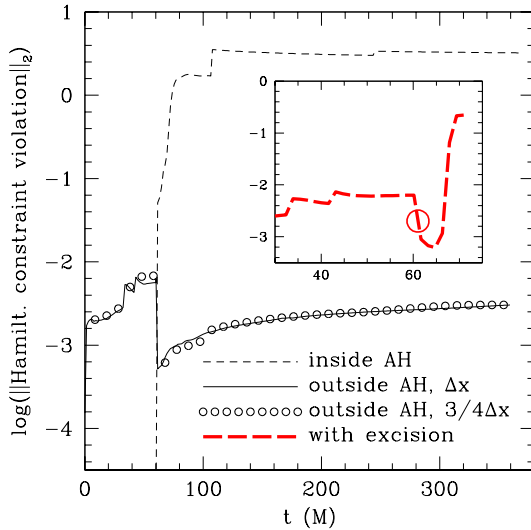


FIG. 2: Evolution of the  $L_2$  norm of the Hamiltonian-constraint violation for model D1. Different curves refer to the violation computed only inside the AH (short-dashed line), only outside it (continuous line) or when the excision is made (long-dashed line in the inset). The circles show the rescaled violation for a higher resolution.

variables and the gauge quantities (No dissipation is introduced for the hydrodynamical variables.). The dissipation is needed mostly because all the field variables develop very steep gradients in the region inside the AH. Under these conditions, small high-frequency oscillations (either produced by finite-differencing errors or by small reflections across the refinement boundaries) can easily be amplified, leave the region inside the AH and rapidly destroy the solution. In practice, for any time-evolved quantity  $u$ , the right-hand-side of the corresponding evolution equation is modified with the introduction of a term of the type  $\mathcal{L}_{\text{diss}}(u) = -\varepsilon \Delta x_i^3 \partial_{x_i}^4 u$ , where  $\varepsilon$  is the dissipation coefficient, which is allowed to vary in space. Indeed, we have experimented with configurations in which the coefficient was either constant over the whole domain or larger for the gridpoints inside the AH. No significant difference has been noticed between the two cases. Much more sensitive is instead the choice of the value of  $\varepsilon$ . In the simulations reported here we have set  $\varepsilon = 0.01$  for model D1 and  $\varepsilon = 0.0075$  for D4, respectively. However, smaller values (e.g.  $\varepsilon = 0.005$ ) are not sufficient to yield the long-term stability discussed here, while larger values (e.g.  $\varepsilon = 0.05$  and  $\varepsilon = 0.01$ , respectively) alter significantly the waveforms, which would not match the ones obtained without dissipation.

As mentioned above, very large gradients in both the space-time and hydrodynamical variables appear soon after the AH formation and they cannot be resolved sufficiently despite the use of several mesh-refinement levels. As a consequence, the solution of the Einstein equations in the region within the AH, becomes increasingly inaccurate as the collapse proceeds. Fig. 2 offers a measure of this loss of accuracy by showing the time evolution of the  $L_2$  norm of the Hamiltonian-constraint violation for model D1. To distinguish the different ampli-

tudes of the errors, the violation has been computed separately for the domain inside the AH and for the rest of the grid.

Several aspects of Fig. 2 are worth noting. Firstly, the two errors are considerably different in amplitude and the one inside the AH increases sharply after horizon formation at about  $t \simeq 60 M$ . Secondly, the sudden decrease in the dashed line at that time is due to the fact that some gridpoints (and in particular those with the largest violations) are no longer included in the calculation of the  $L_2$  norm. Thirdly, the constraint violation outside the AH grows only at a slow pace over the remaining evolution. Finally, shown with circles is the constraint violation for a high-resolution simulation. The values are rescaled to second order before AH formation (when the dominant truncation error comes from hydrodynamics and the HRSC methods used are only second-order) and to third order afterwards (when the smooth accretion flow of the atmosphere boosts the accuracy of the hydrodynamics to third-order). Note that no convergence of the violation is seen inside the AH. Overall, Fig. 2 shows that the solution of the Einstein equations inside the AH is by and large incorrect, but these errors remain confined within the AH and do not contaminate the overall accuracy of the simulation. Shown for comparison in the inset is the constraint violation as computed when the singularity is excised, showing an exponential growth soon after the AH is found and which is marked with a circle.

Note that the ability to perform these long-term evolutions cannot be related in any manner to the use of a “puncture” prescription for the physical singularity, as recently done in simulations of binary black holes [4, 5]. However, it is possible that the stability provided here by the singularity-avoiding gauge and made numerically more robust by the use of dissipation is closely related to the one discussed for punctures [19].

Besides a long-term stability and the possibility of following the collapse well beyond what was possible with the use of excision techniques, the most dramatic advantage produced by the approach suggested here can be appreciated in the study of the gravitational radiation produced during the collapse. As in ref. [9], we have extracted the gravitational-wave information through an approach in which the spacetime is matched with the non-spherical perturbations of a Schwarzschild black hole described in terms of gauge-invariant odd  $Q_{\ell m}^{(o)}$  and even-parity  $\Psi_{\ell m}^{(e)}$  metric perturbations, where  $\ell, m$  are the indices of the angular decomposition. In Fig. 3 we report the lowest-order multipoles  $Q_{20}^+ \equiv \lambda \Psi_{20}^{(e)}$ , where  $\lambda \equiv \sqrt{2(\ell+2)!/(\ell-2)!}$ . The left panel, in particular, shows the signal detected by an observer at a distance of  $42 M$  for the slowly rotating model D1; the right panel, instead, shows the same multipole extracted at  $37 M$  for the rapidly rotating model D4. In both cases the thick lines refer to the evolutions carried out with the excision technique and terminate when the code crashed (cf. left panel of Fig. 1 in ref. [9]). This comparison shows that it is now possible to detect the complete gravitational-wave signal produced by the collapse of a relativistic star to a rotating black hole well beyond what was previously possible in either 2D [20] or 3D

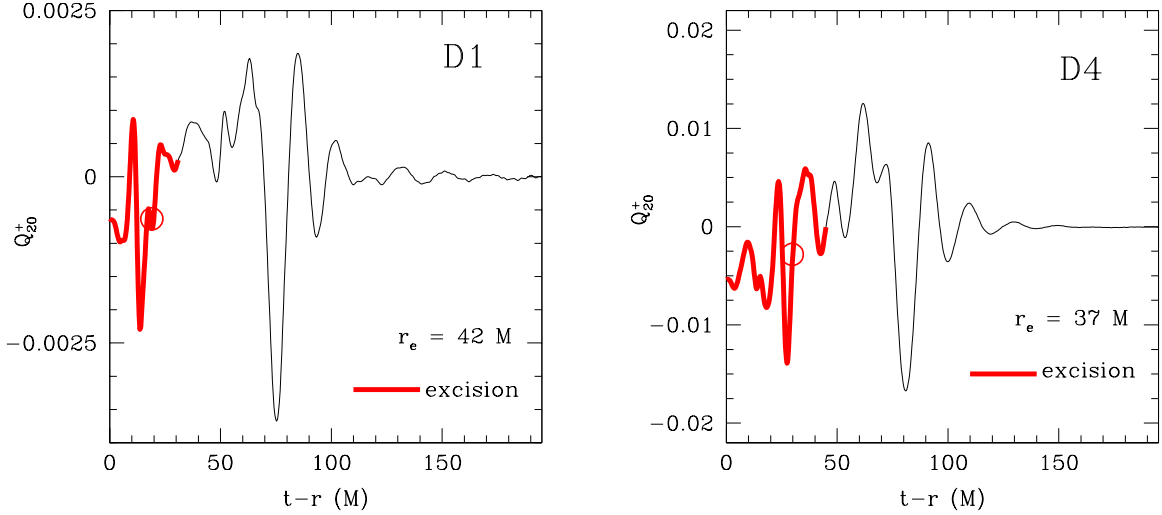


FIG. 3: Lowest gauge-invariant multipole for a slowly rotating star (left panel) and a rapidly rotating one (right panel). Thick lines refer to evolutions carried out with excision and terminate at a code crash, while the circles indicate the time of the AH formation time.

simulations [9]. The estimated error on the phase is  $\lesssim 1\%$  and  $\lesssim 5\%$  on the L2 norm of the amplitude.

Fig. 3 also highlights that the signal can be rather different both in amplitude and form in the two cases with the exception of the final parts, when the signal is dominated by the black-hole QNM ringing. This happens between  $\simeq 80 M$  and  $\simeq 120 M$ , where the signal we extract matches very well with a perturbative one computed using the frequencies given in ref. [21] for the angular momenta and masses of our models. The very good agreement with the perturbative results is an important confirmation of the accuracy of our results which, we recall, are intrinsically plagued by the extreme weakness of the emitted gravitational radiation. Furthermore, the richness of details in the two waveforms opens the prospects that a careful characterization of the waveforms will provide important information on the properties of the black hole as well as of those of the collapsing matter [22].

A straightforward analysis of the *now-complete* gravitational-wave signal computed in these simulations allows us to improve the estimates provided in ref. [9] for the detectability of the gravitational collapse of a uniformly rotating polytropic star at a distance of 10 kpc. More specifically, the total energy lost to gravitational radiation is  $E_{D1} = 3.3 \times 10^{-7} (M/M_\odot)$  for model D1 and  $E_{D4} = 3.7 \times 10^{-6} (M/M_\odot)$  for model D4, with an overall accuracy of  $\sim 10\%$ . The resulting signal-to-noise ratios for these two extremes are then:  $(S/N)_{D1-D4}^{\text{Virgo}} \simeq 0.27 - 2.1$ ,  $(S/N)_{D1-D4}^{\text{advLIGO}} \simeq 1.2 - 11$ , and  $(S/N)_{D1-D4}^{\text{Dual}} \simeq 3.3 - 28$  for detectors such as Virgo/LIGO, advanced LIGO or Dual [23].

In conclusion, we have presented the first 3D calculations of the gravitational collapse of uniformly rotating stars to black holes without excision. This choice, together with suitable gauge conditions and the use of minute numerical dissipation, improves dramatically the long-term stability of the evolutions, providing the most accurate waveforms of this pro-

cess to date. While our approach represents a challenge to the paradigm of singularity excision, it does not necessarily imply that all excision techniques should be expected to lead to instabilities. Rather, it highlights that, for a conformal traceless formulation of the Einstein equations and in highly dynamical spacetimes, the excision of a spherical surface in Cartesian coordinates may be more of a problem than a solution.

We thank D. Pollney, B. Szilágyi and J. Thornburg for useful discussions. Support for this research comes also through the SFB-TR7 of the German DFG and the Italian INFN “OG51”.

---

- [1] G. B. Cook *et al.*, Phys. Rev. Lett. **80**, 2512 (1998).
- [2] T. Nakamura *et al.*, Prog. Theor. Phys. Suppl. **90**, 1 (1987).
- [3] F. Pretorius, Phys. Rev. Lett. **95**, 121101 (2005).
- [4] J. G. Baker *et al.*, Phys. Rev. Lett. **96**, 111102 (2006).
- [5] M. Campanelli *et al.*, Phys. Rev. Lett. **96**, 111101 (2006).
- [6] M. Shibata, Astrophys. J. **595**, 992 (2003).
- [7] M. D. Duez *et al.*, Phys. Rev. D **67**, 024004 (2003).
- [8] E. Schnetter *et al.*, Class. Quantum Grav. **21**, 1465 (2004).
- [9] L. Baiotti *et al.*, Phys. Rev. Lett. **94**, 131101 (2005).
- [10] E. Seidel and W.-M. Suen, Phys. Rev. Lett. **69**, 1845 (1992).
- [11] L. Baiotti *et al.*, Phys. Rev. D **71**, 024035 (2005).
- [12] M. Alcubierre *et al.*, Phys. Rev. D **62**, 044034 (2000).
- [13] L. Baiotti *et al.*, Mem. SAIT, 2003, vol. **1**, p. 327.
- [14] M. Alcubierre *et al.*, gr-qc/0411137, (2004)
- [15] J. Thornburg, Class. Quantum Grav., **21**, 743 (2004)
- [16] C. Bona *et al.*, Phys. Rev. Lett. **75**, 600 (1995).
- [17] M. Alcubierre, Class. Quantum Grav., **20**, 607, (2003).
- [18] H.-O. Kreiss and J. Oliger, GARP Pub. Series **10** (1973).
- [19] M. Hannam *et al.*, gr-qc/0606099 (2006).
- [20] R. F. Stark, T. Piran, Phys. Rev. Lett. **55**, 891 (1985).
- [21] E. Berti *et al.*, Phys. Rev. D **73**, 064030 (2006)
- [22] L. Baiotti *et al.*, *in preparation* (2006)
- [23] M. Bonaldi *et al.*, Phys. Rev. D, **68**, 102004 (2003)
- [24] This is subsequently reduced of 2% to trigger the collapse.